Three-Dimensional Near-Field Microwave Imaging Approach Based on Compressed Sensing

Yang Fang
School of Electronics and Information
Northwestern Polytechnical University
Xi'an, China
E-mail: fang_yang122@sina.cn

Baoping Wang
Science and Technology on UAV Laboratory
Northwestern Polytechnical University
Xi'an, China
E-mail: wbpluo@sina.com

Chao Sun
School of Electronics and Information
Northwestern Polytechnical University
Xi'an, China
E-mail: sunchao13@126.com

***Abstract*—Considering the difficulties in large-scale data processing and low imaging resolution of traditional near-field microwave imaging approach, a new near-field imaging approach based on compressed sensing is proposed in this paper. Under the premise of discretization of imaging scene, the near-field imaging model based on compressed sensing is built firstly. Then the random sparse observation is adopted in the proposed approach to reduce the sampling data volume and improve imaging efficiency, and the optimization reconstruction algorithm is used to obtain an improved higher resolution target image. The effectiveness of this approach is verified through simulation experiment and the microwave anechoic chamber real test experiment. The results show that, compared with the traditional imaging result, the proposed approach in this paper is of higher resolution, even if with a small amount of echo data.**

Keywords—near-field imaging; compressed sensing; sparse observation; planar scanning

I. INTRODUCTION

Microwave near-field imaging, as an effective nondestructive testing and evaluation means, plays an important role in evaluation and detection of critical structures of plane coating, spacecraft and bonding of composite materials, as well as in safety detection of hidden items, as in [1-6]. Since it can provide higher spatial resolution, can realize the relative positioning between sensors and targets, and the system implementation is easily available, it has extensive value in engineering applications.

As for the research on near-field imaging, a lot of work has been done by scholars. J.Fortuny detailed three-dimensional (3-D) near-field SAR imaging technology in his doctoral dissertation, as in [7]; D.Sheen, etc. discussed the application of 3-D near-field imaging technology in nondestructive testing and detection of hidden items, as in [3]; afterwards, S.Li proposed the near-field imaging approach based on Non-uniform Fast Fourier Transform, as in [8,9]. These approaches are all based on the traditional matched filtering technology, and adopt Fourier transform to realize target imaging. Though those approaches can realize target imaging, they have the following problems: traditional imaging system gets target image of higher resolution by obtaining large-scale echo data, but the large-scale data will result in low system testing efficiency, large space of data storage, etc., which bring huge challenges for the engineering application of near-field imaging system. The approach based on matched filtering is a linear process, and does not rely on any prior information of target or the observation area, which resulting in difficulties in breakthroughs in imaging performance and the imaging resolution being restricted by signal bandwidth.

In view of the problems of traditional imaging approach, this paper introduces the theory of compressed sensing (CS) into near-field imaging. First, the near-field imaging model based on CS is built, observation matrix with the optimal reconstruction is designed, and then Separable Surrogate Functionals (SSF) optimization reconstruction algorithm with big data processing capacity is used for target reconstruction. The simulation data of nine points as well as the real test data of five balls can be used to verify the effectiveness of imaging approach in this paper, and Mean Square Error (MSE) index can be adopted to compare the imaging performance of proposed approach with the traditional approach. The results show that the proposed imaging approach has higher imaging resolution in the case of incomplete data.

II. NEAR-FIELD IMAGING MODEL BASED ON COMPRESSED SENSING

3-D discretization should be made for the imaging scene. For convenient representation, the cubic target model is adopted in this paper, as shown in Fig.1. The sampling numbers of probe along x axis and y axis are respectively M and N, and the frequency sampling number is L. The discretization mesh numbers of imaging scene in three directions are respectively P, Q and T. Supposing the signal transmitted as

$$s(t) = \exp(j2\pi ft) \tag{1}$$

After scene discretization, the probe transmits signals to illuminate target scene, and the signals received by probe through target reflection are

$$s(d_i, f) = \sum_{j=1}^{PQT} g(j)\exp[-j4\pi f_l R(d_i, j)/c] \tag{2}$$

wherein, $1 < j < PQT$, $1 < i < MN$, $1 < l < L$, $g(j)$ refers to the reflection coefficient of the mesh jth, f_l refers to the frequency point lth, d_i refers to that the probe is at mesh ith

on scanning plane. $R(d_i, j)$ refers to the distance from scanning position *ith* to target scene *jth*, c refers to velocity of light.

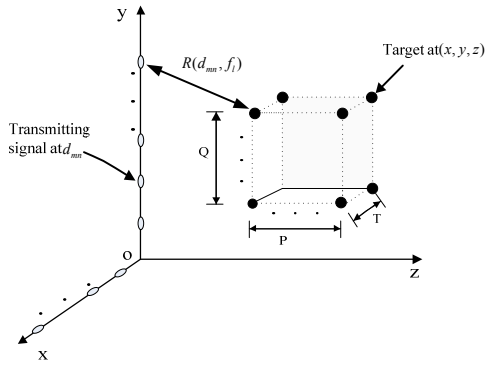

Fig.1. Discretization figure of near-field scanning scene.

The formula (2) refers to the common model of near-field scanning echo signal. To establish the near-field imaging model based on CS, (2) can turn into the following from

$$\mathbf{s} = \mathbf{A}\mathbf{g} \tag{3}$$

wherein, $\mathbf{A}: MNL \times PQT$, $\mathbf{g}: PQT \times 1$, $\mathbf{s}: MNL \times 1$, $\mathbf{s}$ refers to the obtained signal, $\mathbf{A}$ is made up of the mapping relation from target to signal, and $\mathbf{g}$ is made up of the reflection coefficient of target scene. The form of composition of various vectors is

$$\begin{cases} \mathbf{s} = [s(d_1, f_1), \cdots, s(d_1, f_L), \cdots, s(d_i, f_1), \\ \quad \cdots s(d_{MN}, f_1), \cdots, s(d_{MN}, f_L)]^T \\ \mathbf{g} = [g_1, g_2, \cdots, g_{PQT}]^{\mathrm{T}} \\ \mathbf{A} = [\boldsymbol{a}(d_1, f_1), \cdots, \boldsymbol{a}(d_1, f_L), \cdots, \boldsymbol{a}(d_i, f_1), \\ \quad \cdots, \boldsymbol{a}(d_i, f_L), \cdots, \boldsymbol{a}(d_{MN}, f_L)]^T \\ \boldsymbol{a}(d_i, f_l) = [a(d_i, f_l, 1), a(d_i, f_l, 2), \\ \quad \cdots, a(d_i, f_l, PQT)]^T \\ a(d_i, f_l, j) = \exp[-j4\pi f_l R(d_i, j)/c)] \end{cases} \tag{4}$$

III. DESIGN OF IMAGING SCHEME BASED ON COMPRESSED SENSING

In combination of the CS theory, sparse observation mode is adopted, a small number of elements $\mathbf{s}'$ are randomly selected from $\mathbf{s}$ and corresponding rows $\mathbf{A}'$ is selected from matrix $\mathbf{A}$, then the measurement process of CS can be expressed as

$$\mathbf{s}' = \mathbf{A}'\mathbf{g} + \mathbf{n} \tag{5}$$

Wherein, $\mathbf{n}$ refers to noise item. The target image can be obtained by solving the following optimization problems:

$$\begin{cases} \min \|\boldsymbol{g}\|_1 \\ s.t. \ \ \|\mathbf{A}'\mathbf{g} - \mathbf{s}'\|_2 \le \varepsilon \end{cases} \tag{6}$$

A. Sparse observation

To ensure the reconstruction performance, the random observation mode is adopted in this paper, and the observation mode is shown in Fig.2. Fig.2 shows the sampling points are randomly selected on the whole scanning plane for down-sampling observation, and the black points refer to the selected data.

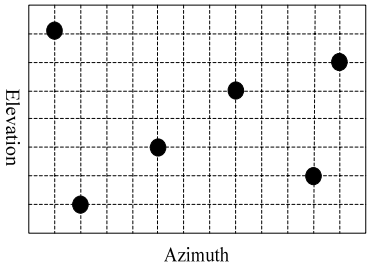

Fig.2. Random observation.

B. Dictionary building

Dictionary matrix is built based on the following formula

$$\mathbf{A}' = \mathbf{F}_{3D}^H \times (\mathbf{E}_{3D}^H \circ \mathbf{F}_{2D}) \tag{7}$$

wherein, $\times$ refers to matrix multiplication, $\circ$ refers to Hadamard product of matrix, and $\mathbf{F}_{2D}$ and $\mathbf{F}_{3D}$ respectively refer to two-dimensional and three-dimensional Fourier transform of reflection coefficient. Matrix $\mathbf{E}_{3D}$ refers to exponential term of match filtering in echo signal in (2), and it is defined as follows

$$\begin{cases} \mathbf{E}_{3D} = \overline{\mathbf{e}} \otimes [1\ 1\ \cdots\ 1]_{1 \times (N_X N_Y N_Z)} \\ \overline{\mathbf{e}} = \begin{bmatrix} e_{(1,1)}^H & e_{(1,2)}^H & \cdots & e_{(1,l)}^H & \cdots & e_{(1,N_Y)}^H \\ \vdots & & & \ddots & & \vdots \\ e_{(N_X,1)}^H & e_{(N_X,2)}^H & \cdots & e_{(N_X,l)}^H & \cdots & e_{(N_X,N_Y)}^H \end{bmatrix}^H \end{cases} \tag{8}$$

the expression of $\mathbf{e}$ is

$$\mathbf{e} = \left[e^{j\sqrt{4k_r^2 - k_x^2 - k_y^2}\, z_0} \right]_{N_X N_Y N_Z} \tag{9}$$

therein, N_x, N_y and N_z respectively refer to the sampling pints along x axis, y axis and z axis. k_r, k_x, k_y respectively refer to the wavenumber along x axis, y axis and z axis. z_0 refer to the distance between scanning plane and the target plane.

C. Reconstruction algorithm

Due to the large volume of near-field scanning three-dimensional imaging data, imaging computation has very strict requirements for computer hardware in case of large number of observation matrix. Since SSF algorithm only involves the multiplication between vector and matrix during imaging computation, extensive matrix inverse operation is saved, and the multiplication of matrixes can be replaced by

FFT. Thus the paper adopts SSF algorithm combining iterative shrinkage and proximal point algorithm.

IV. EXPERIMENTAL VERIFICATION AND ANALYSIS

A. Simulation experiment

Simulation verification is conducted for the imaging algorithm proposed above. The simulation adopts nine points composite target. Four points at the bottom is distributed on the four corners of the cube, the four points on the upper of the cube are located at the middle of four arris, the remaining point is in the center of the cube. And the distribution diagram is shown in Fig.3. Fig.4 shows the target image with complete data when Range Migration Algorithm (RMA) is adopted. Fig.5 shows the imaging results with 60% data when RMA is adopted. Fig.6 shows the imaging results with 60% data when the proposed approach is adopted.

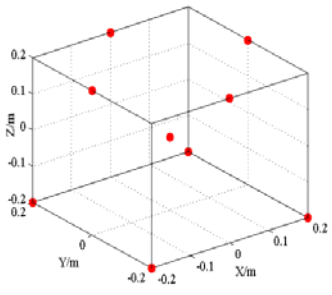

Fig.3. Target model.

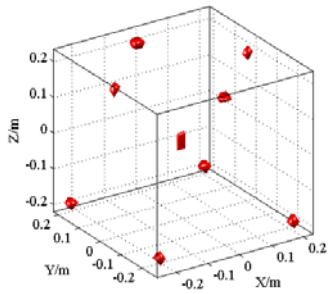

Fig.4. RMA imaging results (complete data).

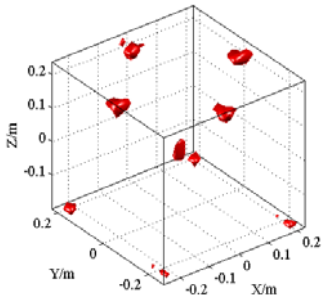

Fig.5. RMA imaging results (60% data).

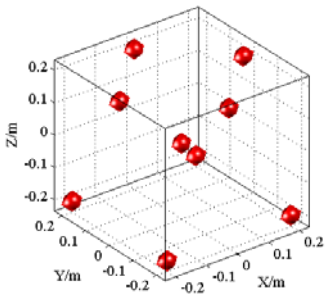

Fig.6. CS imaging results (60% data).

B. Real test experiment

Near-field test platform is built in microwave anechoic chamber to do actual measurement and experimental verification for the proposed approach. The built test system is shown in Fig.7. The testing probe adopted as shown in Fig.8. The test target is the target composed of five metallic balls, as shown in Fig.9. Table I is the test parameters. Fig.10 shows the imaging results with complete data when RMA approach is adopted. Fig.11 shows the imaging results with 12% data when RMA approach is adopted. Fig.12 shows the imaging results with 12% data when CS approach is adopted.

C. Analysis of results

It can be seen from Fig.4 and Fig.10 that, the traditional RMA imaging results are affected by high sidelobe, with low resolution ratio. By comparing Fig.4 and Fig.5, Fig.11 and Fig.12, it can be seen that in the case of defects, there are a

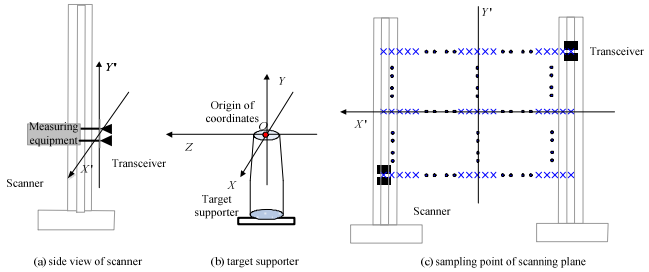

Fig.7. Planar scanning measurement system frame

Fig.8. Scanning frame and probe.

Fig.9. Real picture of five metallic balls.

TABLE I. TESTING PARAMETERS OF FIVE BALLS

Parameters	Symbol	Parameter value
Length of aperture	$L_x \times L_y$	$1m \times 1m$
Antenna scanning interval	Δx , Δy	0.02m，0.02m
Number of scanning points	N_x , N_y	51，51
Signal frequency	f	8GHz-12GHz
Frequency sampling interval	Δf	40MHz
Number of frequency points	N_f	101
Space between scanning plane and target center	d	2m
Transmitting power	W	0dBmw
Scanning speed	V	20mm/s

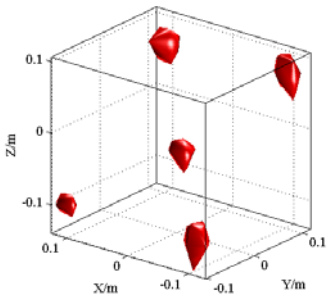

Fig.10. RMA imaging results (complete data).

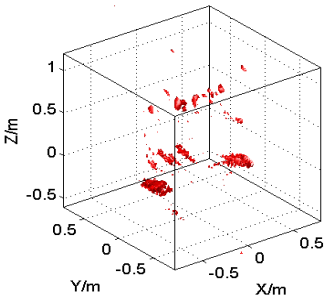

Fig.11. RMA imaging results (12% data).

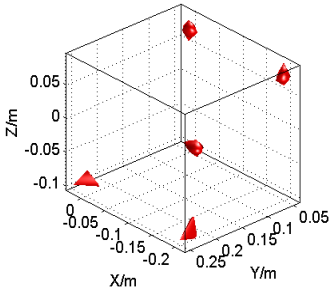

Fig.12. CS imaging results (12% data).

large number of false scattering points in imaging results and images are defocused, then the target cannot be reconstructed in an accurate manner. But the near-field 3-D imaging approach based on CS in this paper not only has the advantages of high resolution ratio and low sidelobe, but also remains good reconstruction effect in case of great defects of echo. The reason is that, in case that data are incomplete and the traditional Nyquist sampling requirements cannot be met, the traditional imaging approach becomes invalid. But the imaging approach based on CS just takes advantages of the sparse information of target echo, and uses optimization algorithm to realize target imaging, so its results are superior to that of traditional imaging. MSE index is adopted below to compare the imaging results of RMA and the proposed approach in this paper. Fig.13 is the comparison curve.

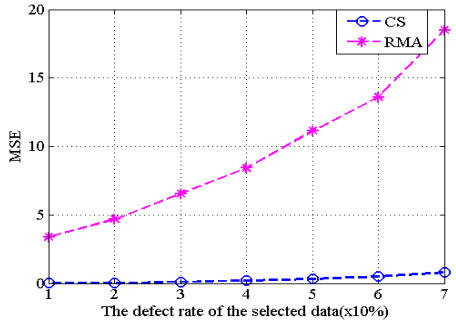

Fig.13. Contrast of RMA and CS imaging.

The vertical axis refers to imaging MSE, while the horizontal axis refers to defect rate of echo data. It can be seen from the figure that, MSE value of traditional imaging is significantly larger than that of the proposed imaging approach in this paper. Along with the increase in missing rate of echo, MSE value of the traditional RMA imaging becomes larger, which indicates that, in the case of incomplete data, the imaging result is significantly superior to the traditional RMA imaging.

V. CONCLUSIONS

With a view to the difficulties of traditional near-field imaging approach in large-scale data processing and low imaging resolution, the near-field imaging model based on CS is built, the random observation matrix is selected as sparse down-sampling matrix, the dictionary corresponding to the imaging model is designed, SSF reconstruction algorithm with big data handling ability is selected, so as to reconstruct target scene. Through simulation experiment and the real test experiment in microwave anechoic chamber, the proposed imaging approach is verified. The experiment results show that, the proposed imaging approach is of higher imaging resolution compared with the traditional imaging approach, and can remain higher resolution in case of incomplete data. Finally, the performance index of MSE is used to compare the imaging results of the proposed imaging approach and that of the traditional imaging result. The original contribution of this paper are follows:

1） The uniform imaging model of planar scanning based on CS is built in this paper.

2） Random observation down-sampling and SSF algorithm used for processing large-scale data are used in CS-based near-field imaging.

3） The experimental data is obtained in the microwave anechoic chamber with near-field test platform, and a higher resolution target image is obtained by using the proposed imaging approach.

Next, it is to design the observation matrix beneficial for hardware implementation and optimization reconstruction, so as to achieve rapid near field target RCS measurement and high-precision imaging result. In addition to this, in the actual imaging system, phase error exists in echo signal due to external factors. For near-field scanning 3-D imaging, the major consideration is the phase error in the azimuth (two directions that probe move) caused by the movement of the probe. In order to get a high focusing image, it is necessary to compensate the phase error.

ACKNOWLEDGMENT

This work was supported in part by the National Natural Science Foundation of China (NSFC) under Grant 61472324. The authors would like to thank the heading editor and the anonymous reviewers for their valuable and helpful comments.

REFERENCES

[1] S. Kharkovsky, R. Zoughi, “Microwave and millimeter wave nondestructive testing and evaluation-overview and recent advances,” IEEE Instrumentation & Measurement Magazine, vol. 10, pp.26-38, April, 2007.

[2] D.M.Sheen, D.L.McMakin, and T.E.Hall, “Three-dimensional millimeter-wave imaging for concealed weapon detection,” IEEE Transactions On Microwave Theory And Techniques, vol.49, pp. 1581-1591, September, 2001.

[3] D.Sheen, D.McMakin, and T.Hall, ‘Near-field three-dimensional radar imaging techniques and applications,’ Applied Optics, vol.49, pp. 83-93, July, 2010.

[4] H.D.Collins, D.L.McMakin, T.E.Hal, and R.P.Gribble, ‘Real-time holographic surveillance system,’ U.S Patent, 5455590, October, 1995.

[5] D.M.Sheen, H.D.Collins, T.E.Hall, D.L.McMakin, R.P.Gribble, Severtsen R H, Prince J M, Reid and L D, ‘Realtime wideband holographic surveillance system,’ U.S. Patent, 5557283, September, 1996.

[6] Z.Yang , Y.R.Zheng, ‘Near-field 3-D synthetic aperture radar imaging via compressive sensing,’ International Conference on Acoustics, Speech and Signal Processing, pp. 2513-2516, 2012.

[7] J.Fortuny. ‘Efficient Algorithms for Three-Dimensional Near-Field Synthetic Aperture Radar Imaging,’ Faculty of Electrical Engineering University of Karslruhe, Germany, 2001.

[8] S.Li, B.Zhu and H.Sun, ‘NUFFT-Based Near-Field Imaging Technique for Far-Field Radar Cross Section Calculation,’ IEEE Antennas and Wireless Propagation Letters, vol. 9, pp. 550-553, May, 2010.

[9] S.Li, H.Sun, B.Zhu, and R.Liu. ‘Two-Dimensional NUFFT-Based Algorithm for Fast Near-Field Imaging,’ IEEE Antennas and Wireless Propagation Letters, vol. 9, pp. 814-817, August, 2010.